The 2006 Eruption of Augustine Volcano, Alaska
Power, J.A., Coombs, M.L., and Freymueller, J.T., editors
U.S. Geological Survey Professional Paper 1769

Chapter 21

Volcanic-Ash Dispersion Modeling of the 2006 Eruption of Augustine Volcano Using the Puff Model

By Peter W. Webley[1], Kenneson G. Dean[1], Jonathan Dehn[1], John E. Bailey[1,2], and Rorik Peterson[3]

Abstract

Volcanic ash is one of the major potential hazards from volcanic eruptions. It can have both short-range effects from proximal ashfall and long range impacts from volcanic ash clouds. The timely tracking and understanding of recently emitted volcanic ash clouds is important, because they can cause severe damage to jet aircraft engines and shut down major airports. Dispersion models play an important role in forecasting the movement of volcanic ash clouds by being the only means to predict a clouds' trajectory. Where available, comparisons are possible to both remote-sensing data and observations from the ground and aircraft. This was demonstrated in January 2006, when Augustine Volcano erupted after about a 20-year hiatus. From January 11 to 28, 2006, there were 13 explosive events, with some lasting as long as 11 minutes and producing ash clouds as high as 10–12 km (33,000–39,000 ft) above mean sea level (a.m.s.l). From January 28 to February 4, 2006, there was a more continuous phase, with ash clouds reaching 4–5 km a.m.s.l (13,000–16,000 ft). During the eruption, the Puff dispersion model was used by the Alaska Volcano Observatory for trajectory forecasting of the associated volcanic ash eruption clouds. The six explosive events on January 13 and 14, 2006, were the first time the "multiple eruptions" capability of the Puff model was used during an eruption response. Here we show the Puff model predictions made during the 2006 Augustine eruption and compare these predictions to satellite remote-sensing data, Next Generation Radar (NEXRAD) radar, and ashfall measurements. In addition, we discuss how automated predictions for volcanoes at elevated alert status provide a quicker assessment of the risk from the potential ash clouds.

[1]Alaska Volcano Observatory, Geophysical Institute, University of Alaska Fairbanks, 903 Koyukuk Drive, Fairbanks, AK 99775.

[2]Now at: Scenarios Network for Alaska Planning, University of Alaska Geography Program, Fairbanks, AK 99775.

[3]Department of Mechanical Engineering, University of Alaska Fairbanks, P.O. Box 755905, Fairbanks, AK 99775.

Introduction

Volcanoes can inject large volumes of ash into the atmosphere, posing a threat to international and domestic aircraft as well as disrupting local communities. Ash clouds can cause severe damage to jet aircraft engines and fuel lines, abrade aircraft internal and external surfaces and shut down major airports (Blong, 1984; Casadevall, 1993; Casadevall and Krohn, 1995; Miller and Casadevall, 2000). The North Pacific (NOPAC) region is a vast expanse, 5,000 km by 2,500 km, containing numerous active volcanoes, most of which are located in uninhabited areas along the Aleutian Islands and Kamchatka Peninsula, Russia (fig. 1). From 1975 to 2006, there were more than 200 separate volcanic ash clouds that reached at least 6 km (20,000 ft) above mean sea level (a.m.s.l) and potentially jeopardized aircraft safety. Within the NOPAC region, the agencies responsible for monitoring volcanoes and their associated eruptions are: Alaska Volcano Observatory (AVO), Kamchatka Volcano Emergency Response Team (KVERT), and Sakhalin Volcanic Eruption Response Team (SVERT) who work together with the Tokyo, Washington and Anchorage Volcanic Ash Advisory Centers (VAAC) to provide advisories of airborne volcanic ash. These advisories are used by the local meteorological watch offices to provide a Significant Meteorological Information (SIGMET) warning to the aviation community and volcanic ashfall warnings to local communities.

Volcanic Ash Transport and Dispersion (VATD) models play an important role in forecasting the movement of volcanic ash clouds and provide information that is otherwise difficult or impossible to collect from other data sources. When remote-sensing data and observations from the ground and aircraft are available, these model predictions can be compared and validated. Before, and in the initial stages of volcanic eruptions, VATD models are invaluable in predicting the movement of volcanic ash clouds and ensuring aviation safety. A warning system should be capable of a 5-minute response time once an eruption has been detected (Hufford and others, 2000). During these initial minutes, predicting the movement of the ash cloud and the potential impacts on aircraft are critical. Within Alaska, AVO's level of response to remote volcanic activity varies depending on the source and content of the observation. After receiving a report of an eruption, AVO works with the National Weather Service (NWS) and Federal Aviation Administration (FAA) for corroboration and to solicit additional information. AVO itself is a joint program of the United States Geological Survey (USGS), the Geophysical Institute of the University of Alaska Fairbanks (UAF-GI) and the State of Alaska Division of Geological and Geophysical Surveys (ADGGS).

VATD models provide the only means to quantitatively predict an ash cloud's trajectory. There are three VATD models often used for forecasting ash cloud motion in the NOPAC region: Canadian Emergency Response Model (CanERM: Pudykiewicz, 1988, 1989), Hybrid Single-Particle Lagrangian Integrated Trajectories (HYSPLIT: Draxler and Hess, 1997, 1998), and Puff (Searcy and others, 1998). Peterson and others (2010) provide a detailed description

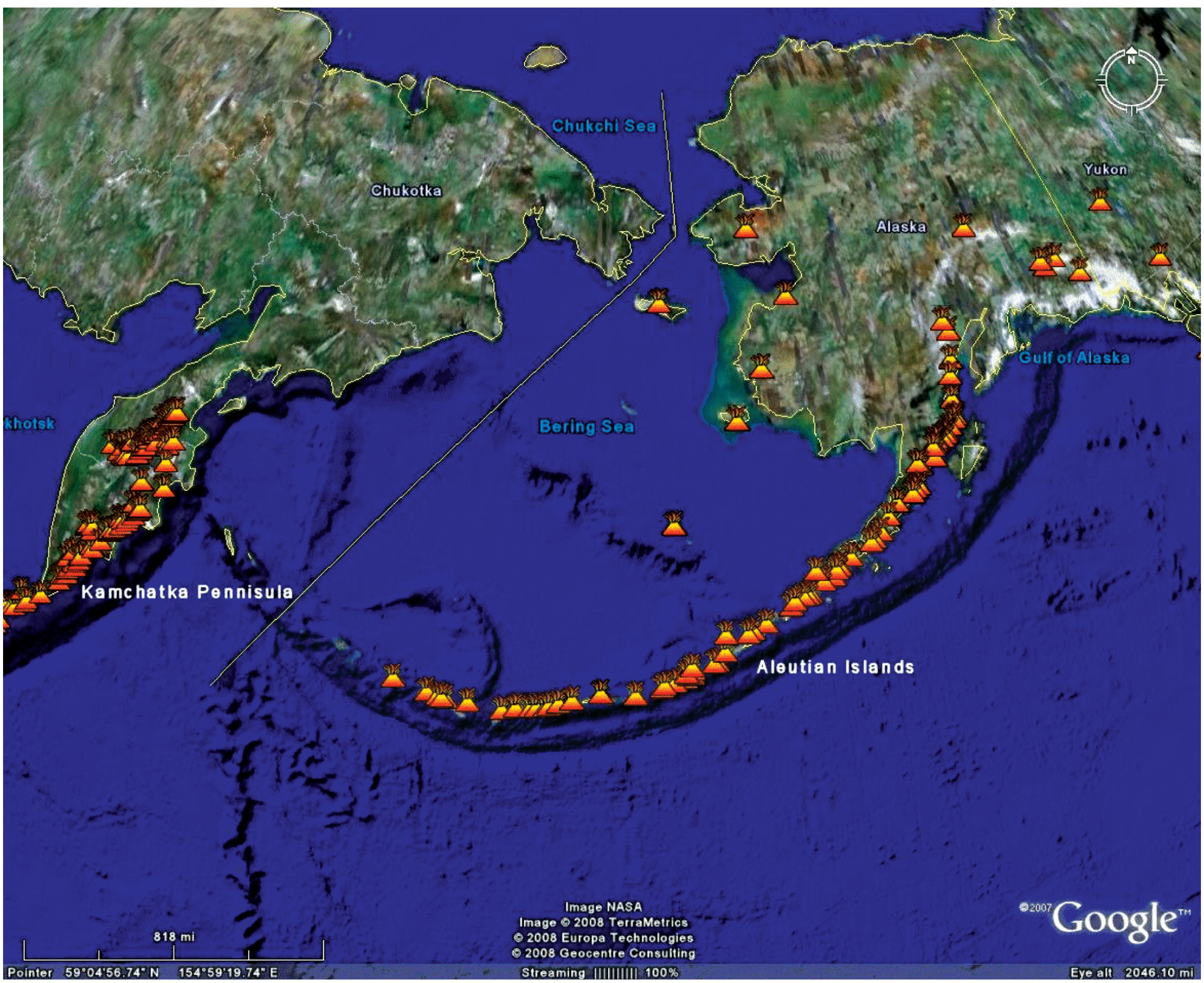

Figure 1. Map of North Pacific region, illustrating the numerous volcanoes (colored triangles) from Kamchatka in the west to the Alaska mainland and Canada in the east (image courtesy of Google Earth).

of all three models. Puff is primarily focused on forecasting volcanic ash transport and dispersion using an adjustable number of tracer particles to represent a volcanic ash cloud. The model is designed to rapidly predict the extent and movement of airborne ash particles during an eruption (Searcy and others, 1998). Model simulations place hypothetical particles above a selected volcano, release them into a gridded wind field and calculate their movement. Current numerical weather prediction (NWP) model forecasts are used for real-time predictions.

Puff is used at AVO, Anchorage and Washington VAACs, the Airforce Weather Agency (AFWA), and other national agencies and universities worldwide. The Puff model has been used as a VATD model for numerous volcanic eruptions in the North Pacific. The first use of the model was during the eruption of Redoubt Volcano in 1989–90 (Tanaka, 1994). Searcy and others (1998) demonstrated the model's use by comparing predictions to satellite images of the eruptions of Crater Peak at Mount Spurr in 1992 and of Klyuchevskoi Volcano in 1994. Dean and others (2002) predicted the movement of the ash cloud from the 2001 eruption of Cleveland Volcano and showed possible limitations of satellite data when compared to the model predictions, and Aloisi and others (2002) used the model to analyze the July 1998 eruption cloud from the Mount Etna paroxysm. Additionally, Papp and others (2005) investigated the probability of ash distribution in the NOPAC based on multiple, hypothetical eruptions over several years, and Peterson and others (2010) compared model predictions from Puff, HYSPLIT, and CanERM for selected eruptions in the NOPAC.

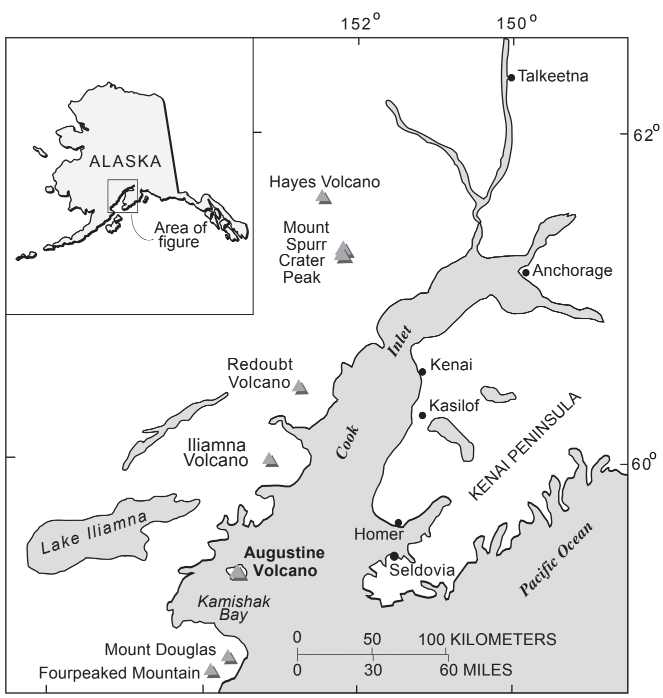

Figure 2. Map showing location of Augustine Volcano, in Cook Inlet, southwest of Anchorage, Alaska. Grey triangles show the locations of the volcanoes within this region of Alaska.

Most recently, the Puff model was used in January 2006, when Augustine Volcano (fig. 2) reawakened and over a period of 20 days produced 13 explosive eruptions, followed by a period of continuous ash emission. The 2006 eruption was preceded by approximately 8 months of increasing unrest that included escalating seismic activity, deformation of the volcanic edifice, gas emission, and small phreatic explosions (Power and others, 2006). The eruption progressed through four phases. In May 2005, the volcano started a precursory phase with increasing microearthquakes (Power and others, 2006). From January 11 to 28, 2006 the volcano was in an explosive phase characterized by 13 discrete explosions, followed by a more continuous phase of lesser explosivity and lava effusion from January 28 through February 10 and concluding with an effusive phase from March 3 to 15 (Coombs and others, this volume).

In this paper, we show the use of the Puff model during the 2006 eruption of Augustine Volcano. New modeling capabilities are introduced, many of which were used for the first time during an eruption response, with validation of these model simulations. Also shown is how the frequency of the explosive events at Augustine led to both new developments and new data-visualization tools. We compare the Puff model simulations to satellite data and ashfall measurements to assess the reliability of the eruption response predictions. We describe the Puff model's use by separating the explosive phase into three parts on the basis of the timings of the events: (1) January 11, (2) January 13 and 14, and (3) January 17, with the early part of the following continuous phase as one period, (4) January 28 to February 2, 2006.

The 2006 Eruption at Augustine Volcano

The 2006 eruption of Augustine Volcano was preceded by increased seismicity beginning in May 2005. By January 11, 2006, there were significant satellite detected thermal anomalies and strong seismic signals, and on that day two explosions occurred, each lasting less than 4 minutes (Power and others, 2006). The January 11 explosions produced ash plumes, reported by NWS to have reached heights greater than 9 km a.m.s.l. (approximately 30,000 ft), which moved slowly to the north and northeast (Power and others, 2006). On January 13, a third explosive event occurred, which lasted for 11 minutes and produced volcanic plumes/ash clouds detected to 10 km (33,000 ft) a.m.s.l. During January 13, there were five discrete events, followed by events on January 14 and 17 (see table 1). Figure 3*A* is a time-lapse camera image from Augustine Island that shows that the events on January 13 were ash rich, and by January 28, the continuous-phase eruptions were a mixture of steam, gases and some ash (fig. 3*B*).

In response to these explosive eruptions, the Puff model was used by AVO to track and predict the movement of the volcanic ash clouds. The model simulations were compared with all available satellite remote-sensing data. During the 2006 eruption, satellite data were available from the Advanced Very High Resolution Radiometer (AVHRR) on the National Oceanic and Atmospheric Administration (NOAA) satellites, the Moderate Resolution Imaging Spectroradiometer (MODIS) on National Aeronautics and Space Administration (NASA) Terra and Aqua satellites and the NOAA Geostationary Operational Environmental satellites (GOES). Bailey and others (this volume) provide a description of the data for both thermal monitoring and the detection of the volcanic ash clouds. On January 28, the volcano entered a period of more continuous eruptive activity that lasted until February 2. This phase began with four explosive eruptions that generated ash plumes up to 9 km (30,000 ft) a.m.s.l (Power and others, 2006). Ash plumes ascended to 4 km (~13,000 ft) a.m.s.l. frequently during the continuous phase. Winds carried ash to the south, depositing trace amounts on Kodiak Island and interrupting air traffic at the Kodiak Airport, and then carried ash north across Alaska (Webley and others, 2008).

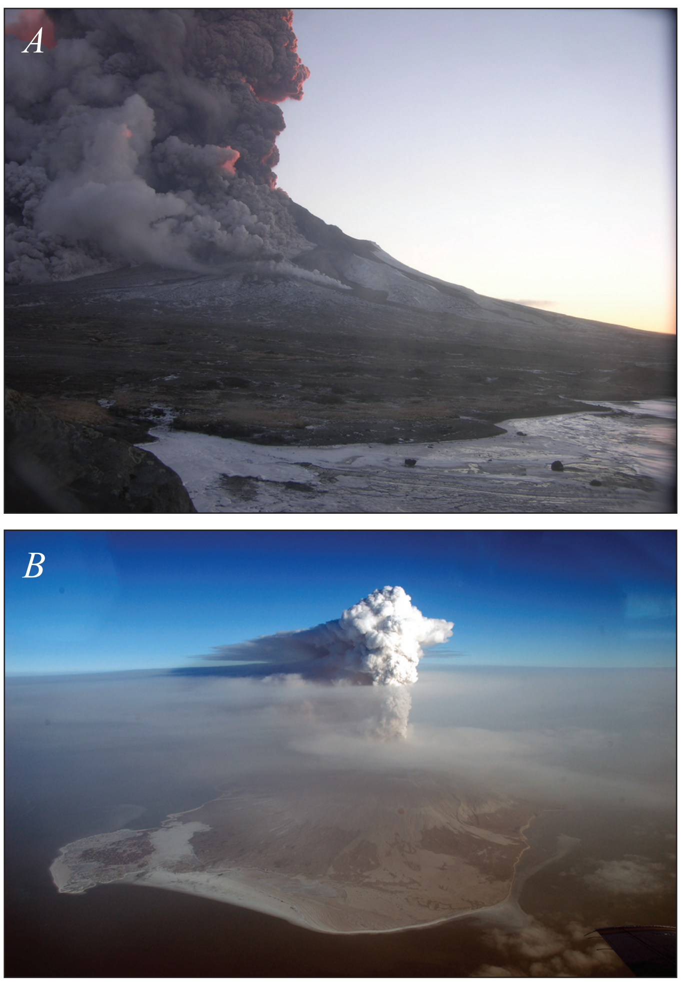

Figure 3. Photographs of Augustine Volcano's 2006 eruption. *A*, Time lapse camera image taken on January 13, 2006, from a site at Burr Point, 5 km north of Augustine's summit (Paskievitch and others, this volume). *B*, Oblique aerial photograph of a steam plume with minor ash, extending northeast from Augustine Volcano on January 30, 2006. The view is from southwest. AVO photo by R.G. McGimsey.

Puff Model Simulations

At AVO, once a volcanic event was confirmed, the Puff model was used to predict the movement of the subsequent ash cloud for the following 24-hour period. Initially, several assumptions were made for the plume height, eruption duration, particle-size distribution, and vertical distribution of the ash particles in the plume. As more information became available, the model prediction was updated to provide a better representation of the ash cloud movement. The Puff model uses numerical weather prediction (NWP) forecasts for its advective term when predicting the future movement of a volcanic cloud trajectory. During the Augustine eruption, the North American Mesoscale model (NAM) domain 216 was used; this is a 32-km spatial resolution data set. Additional NWP forecasts were available from the Weather Research Forecast (WRF) model at 1.67-km and 5-km spatial resolutions. However, this was an experimental data set and so was not used during the eruption response.

For this paper, AVHRR channel 4 (10.2–11.2 micron) and channel 5 (11.5–12.5 micron) data were used to detect ash clouds, including generating "split window" images, using the reverse absorption method, first noted by Prata (1989a, b). AVHRR channel 4 data are useful for detecting opaque ash clouds (Dean and others, 2002) and the reverse absorption method becomes a useful tool once the ash clouds are "semi-transparent". Here we use the reverse absorption method through a brightness temperature difference (BTD) of the infrared channels as stated by Prata (1989a). Eruption clouds early on in their development can fail to allow discrimination of ash, given that they are spectrally opaque (Wen and Rose, 1994; Krotkov and others, 1999; Simpson and others, 2000). Part of the ash cloud needs to be "translucent", which indicates a low optical depth, for the reverse absorption method to be successful. The ash signal can be affected by water vapor in the atmosphere, which can cause the signal sometimes to become slightly negative, even there is not ash present in the atmosphere (Simpson and others, 2000; Prata and others, 2001; Simpson and others, 2001). Additionally, ice within volcanic clouds can cause the reverse absorption method to be ineffective (Rose and others, 1995).

January 11, 2006

On January 11, 2006, Augustine Volcano had two explosive events at 0444 and 0512 Alaska Standard time (AKST; 1344 and 1412 UTC), as much as 3 minutes 13

Table 1. Volcanic eruption parameters for Augustine's 2006 explosive and continuous phases, as used by the Puff model.

[All heights a.m.s.l . UTC = coordinated universal time, AKST = Alaska Standard Time, Jan = January, Feb = February, km = kilometers, ft = feet, s = seconds, min= minutes. AKST = UTC – 9 hours. Note that the start and end times of the eruptive events were determined from AVO seismic stations]

Event No.	Date	Start Time (AKST)	End Time (AKST)	Duration	Plume Height[1]	Plume Height[2]
1	11 Jan 2006	04:44:00 (13:44:00 UTC)	04:45:18 (13:45:18 UTC)	1 min 18 s	30,000 ft (~9 km)	6.5 km
2	11 Jan 2006	05:12:00 (14:12:00 UTC)	05:15:18 (14:52:18 UTC)	3 min 18 s	28,000 ft (~8.5 km)	10.2 km
3	13 Jan 2006	04:24:00 (13:24:00 UTC)	04:35:00 (13:35:00 UTC)	11 min	34,000 ft (~ 10.4 km)	10.2 km
4	13 Jan 2006	08:47:00 (17:47:00 UTC)	08:51:17 (17:51:17 UTC)	4 min 17 s	30,000 ft + (~ 9 km+)	10.2 km
5	13 Jan 2006	11:22:00 (20:22:00 UTC)	11:25:24 (20:25:24 UTC)	3 min 24 s	36,000 ft + (~ 11 km+)	10.5 km
6	13 Jan 2006	16:40:00 (1/14 01:40:00 UTC)	16:44:00 (1/14 01:44:00 UTC)	4 min	34, 000 ft + (~ 10.4 km+)	10.5 km
7	13 Jan 2006	18:58:00 (1/14 03:58:00 UTC)	19:01:00 (1/14 04:01:00 UTC)	3 min	30,000 ft (~ 9 km)	13.5 km
8	14 Jan 2006	01:14:00 (09:14:00 UTC)	01:17:00 (09:17:00 UTC)	3 min	~ 30,000 ft (~ 9 km)	10.2 km
9	17 Jan 2006	07:58:00 (16:58:00 UTC)	08:02:11 (17:02:11 UTC)	4 min 11 s	45,000 ft (~ 13.7 km)	13.5 km
10	27 Jan 2006	20:24:00 (1/28 05:24:00 UTC)	20:33:00 (1/28 05:33:00 UTC)	9 min	30,000 ft (~ 9 km)	10.5 km
11	27 Jan 2006	22:37:21 (1/28 08:37:21 UTC)	22:38:45 (1/28 08:38:45 UTC)	1 min 2 s	< 10,000 ft (< 3 km)	3.8 km
12	28 Jan 2006	02:04:13 (11:04:13 UTC)	02:06:40 (11:06:40 UTC)	2 min 6 s	26,000 ft (~ 8 km)	7.3 km
13	28 Jan 2006	07:42:00 (16:42:00 UTC)	07:45:00 (16:45:00 UTC)	3 min	25,000 ft (~ 7.6 km)	7 km
continuous phase	28 Jan 2006	14:30:00 (23:30:00 UTC)	1 Feb 2006	4 days	10,000 – 14,000 ft [3] (~ 3 – 4.3 km)	3.8 km [4]

[1]Eruption response plume height from NWS.

[2]NEXRAD radar plume height.

[3]Discrete events to 30,000 ft.

[4]Discrete events to 7.2 km. 1 km = 3,280 ft.

seconds in duration, and that produced ash clouds of 8–9 km a.m.s.l. (26,000–30,000 ft) (table 1). Once the explosions were detected by the AVO seismic network, the Puff model was implemented to predict the movement of the emitted ash clouds using a default plume height of 16 km a.m.s.l (52,000 ft), to ensure that the full eruption column was included. For these two events, Puff predicted very similar patterns in both simulations (fig. 4): a spiral-shaped ash cloud with the ash above 6 km (20,000 ft) a.m.s.l drifting mostly east away from Augustine and across the Kenai Peninsula and the lower ash, < 6 km a.m.s.l, drifting mostly north. Initially, an opaque ash cloud was detected by satellite data (fig. 5*A*). Once translucent, this ash cloud was detectable by the reverse absorption method (fig. 5*B*), with

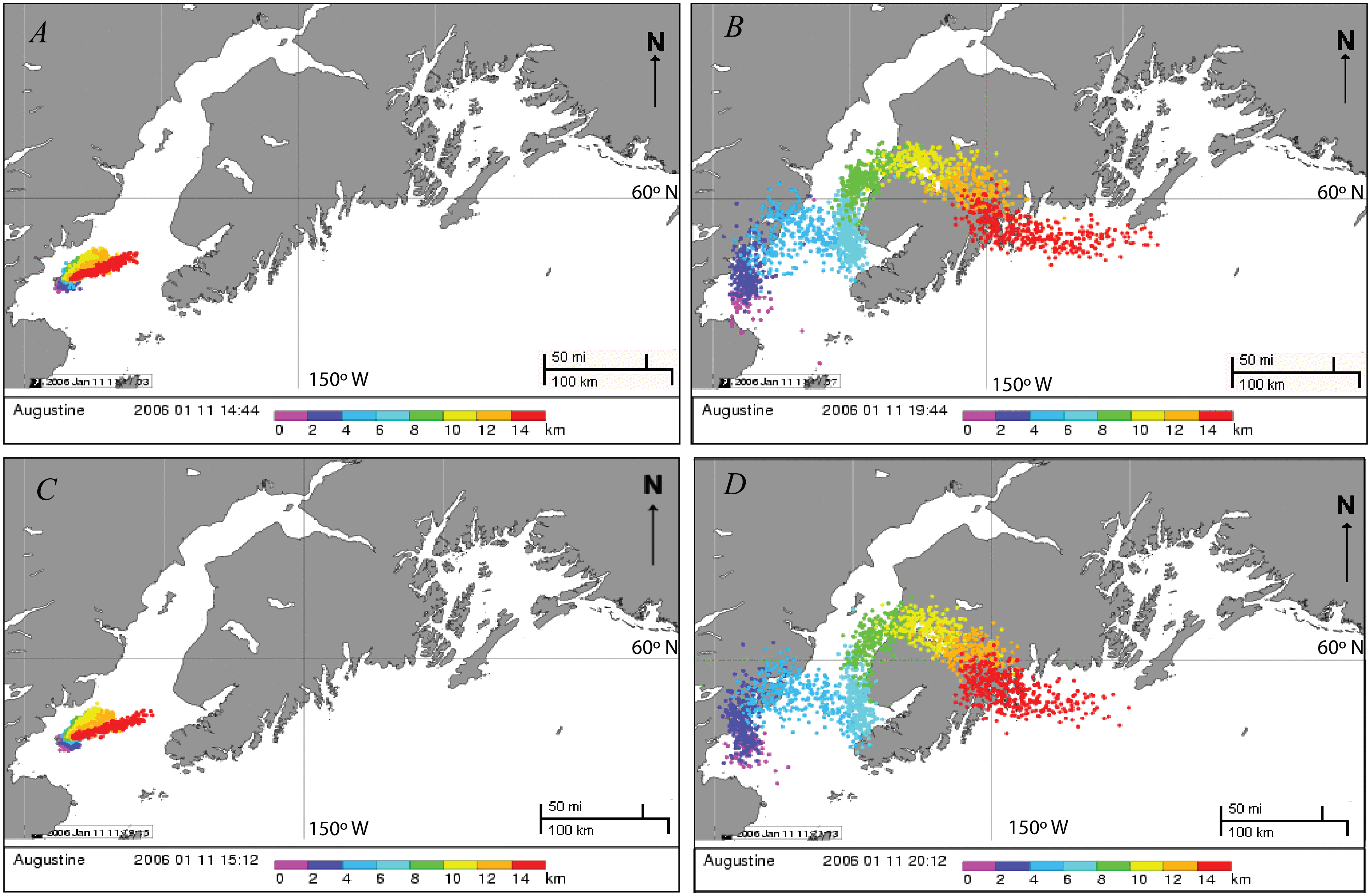

Figure 4. Puff eruption response simulations for the January 11, 2006 explosions. *A* and *B* for the first event at 0444 AKST (1344 UTC) eruptions at +1 and +6 hours. *C* and *D* are for the second event at 0512 AKST (1412 UTC) eruption at +1 and +6 hours. Times are in UTC, and particles are color-coded by elevation a.m.s.l.

a negative brightness temperature difference (BTD) signal. For these two events on January 11, the ash cloud was only detectable in a few satellite images. The NWS tracked the plume moving north towards the west side of Cook Inlet, corresponding to the low level sections of the Puff forecast below 6 km a.m.s.l. The explosive events on January 11 showed little ash in the satellite data, consistent with interpretation of seismic signals from the events, which suggest the explosions were mostly caused by gas release (McNutt and others, this volume).

January 13–14, 2006

Starting at 0424 AKST (1324 UTC) on January 13, Augustine Volcano had six further explosive events. On the basis of the AVHRR satellite sensor data, the events on January 13 and 14 (fig. 6) showed a stronger ash signal than seen for the second explosive event on January 11 (fig. 5). The first event on January 13 started at 0424 AKST (1324 UTC), had an 11-minute duration, and produced an ash cloud that ascended to approximately 10 km a.m.s.l (33,000 ft) (table 1). Within approximately 24 hours, there would be five more explosive events lasting around 3 to 4 minutes each, and producing ash columns from 9 to 11 km a.m.s.l (30,000–36,000 ft) (table 1). The movements of ash clouds from these events were predicted and simultaneously tracked using the "multiple eruption" option in the Puff model. This was the first time that this tool had been applied during an eruption response. The tool allows Puff to predict the movement of many volcanic ash clouds at one time. As each of the six events was confirmed, the model predictions were then updated. For each new prediction, the Puff model integrated the new and older ash clouds to track all of them together, so all six plumes' movements were forecasted simultaneously. These forecasts were then compared to any additional data once available.

Figure 6 shows the volcanic ash plumes detected on several AVHRR satellite images during January 13–14. Figure 6*A* shows the first plume at 0609 AKST (1509 UTC) on January 13 drifting east across Cook Inlet towards the Kenai Peninsula. Figure 6*B* shows that there were two ash plumes detectable in the satellite data at 1024 AKST (1924 UTC). The first was over the Kenai Peninsula, with a weak ash signal, and the second was to the east of Augustine Volcano, in Cook Inlet. Figure 6*C* shows three detected ash clouds at 1203 AKST (2103 UTC) that moved in an east-northeast direction. By 2020 AKST on January 13 (0520 UTC on January 14), these first three plumes had dispersed and moved out into the Gulf of Alaska. Figure 6*D* shows the fourth and fifth plumes (events 6 and 7 in table 1), which moved in a more south-easterly direction, through the strait between the Kenai Peninsula and Kodiak Island and out into the Gulf of Alaska, with the strongest ash signal at the

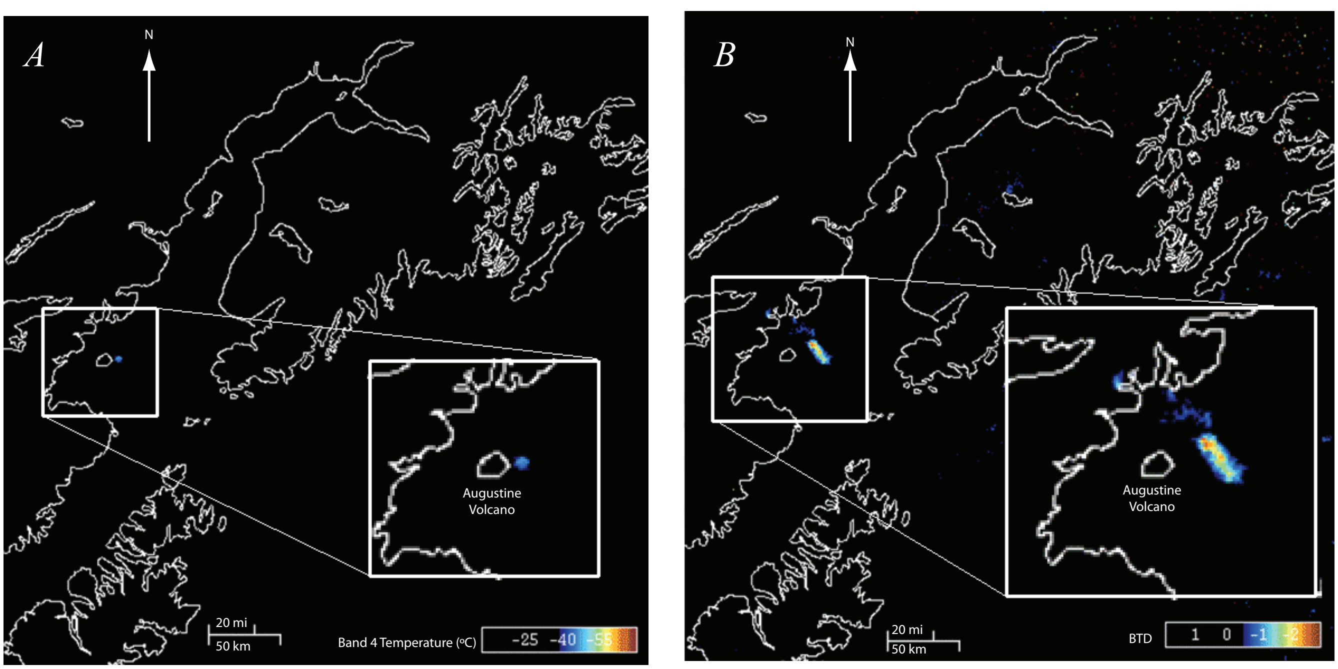

Figure 5. Advanced Very High Resolution Radiometer (AVHRR) satellite sensor data as images from January 11, 2006. *A*, Opaque ash cloud at 0448 AKST (1348 UTC). *B*, Ash signal, shown as brightness temperature differences (BTD), at 0659 AKST (1559 UTC). BTD scale is difference in AVHRR channels 4 and 5 using the reverse absorption method.

"head" of the ash clouds. Additional discussion of the satellite data collected on January 13–14 is included in Bailey and others (this volume). Figure 7 shows time-snapshots during the Puff model forecasts of the six plumes (events 3 to 8 in table 1) from January 13–14 as they drift across the Gulf of Alaska. The simultaneous forecast of the movement of these multiple ash clouds simplified a very complex geographic problem of displaying and accounting for all of the ash clouds at one given time and demonstrated that we can track and forecast all of them to make a hazard assessment.

Figure 8 shows a comparison of the Puff eruption response forecasts to the AVHRR satellite sensor data

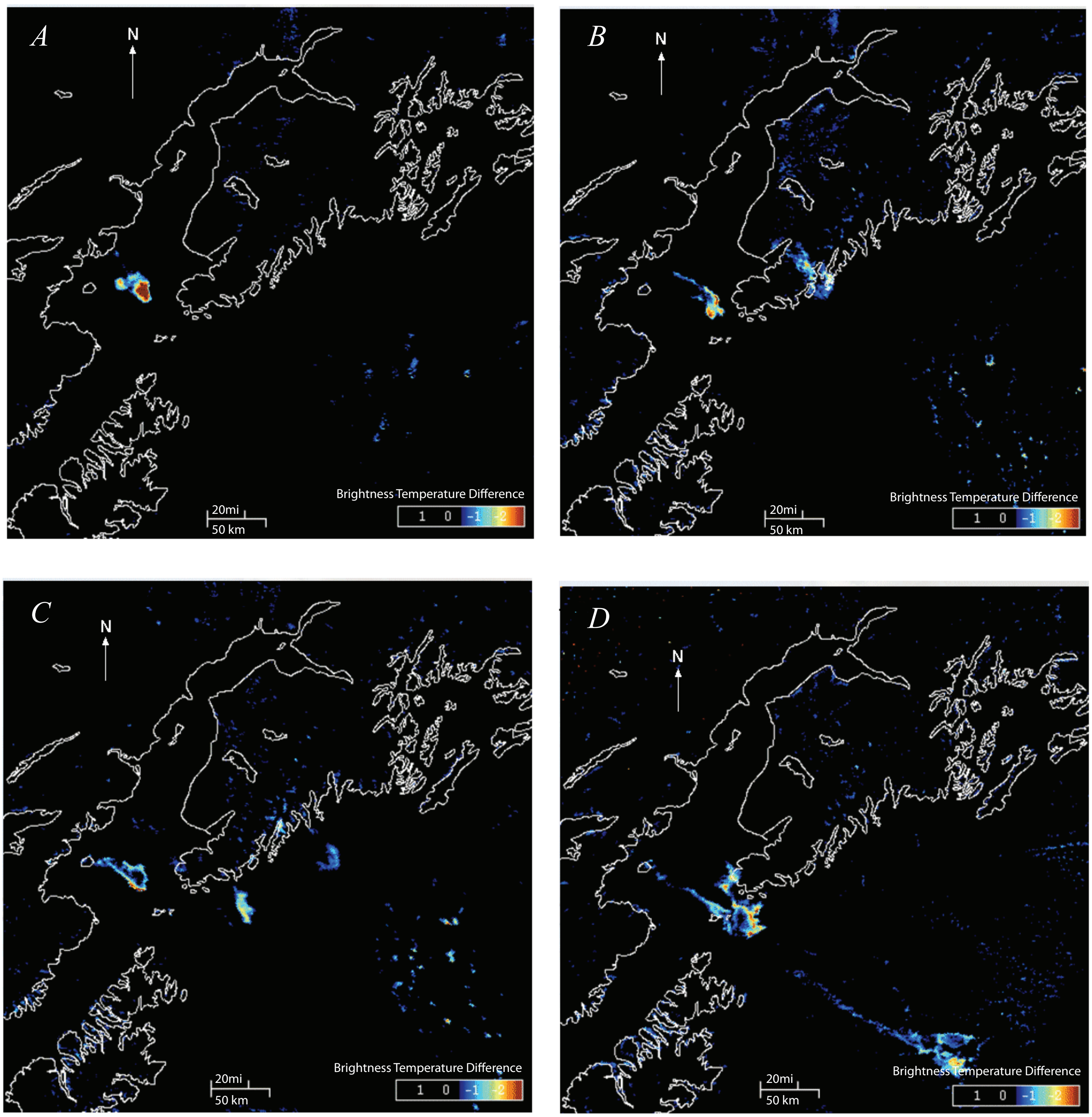

Figure 6. Time-snapshot series of the multiple plumes from Advanced Very High Resolution Radiometer sensor satellite data using reverse absorption method, BTD, on January 13, 2006. *A*, 0609 AKST (1509 UTC). *B*, 1024 AKST (1924 UTC). *C*, 1203 AKST (2103 UTC). *D*, 2020 AKST (0520 UTC on 14 January 2006). BTD scale is difference in AVHRR channels 4 and 5 using the reverse absorption method.

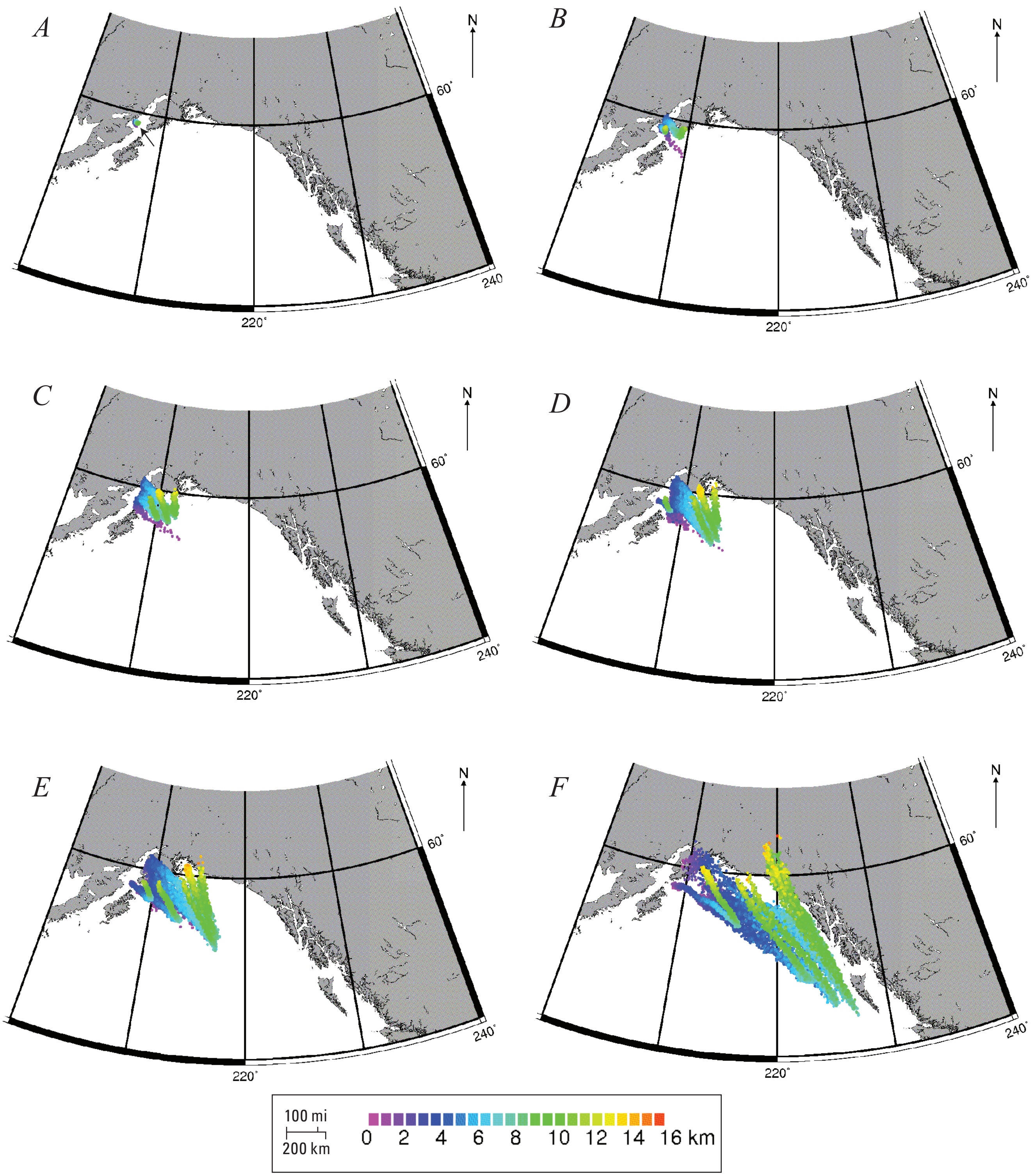

Figure 7. Time snapshots during the 24 hour Puff simulations from the six plumes during January 13–14, 2006. *A*, January 13 at 0520 AKST (1420 UTC). *B*, January 13 at 1020 AKST (1920 UTC). *C*, January 13 at 15:20 AKST (14 January at 0020 UTC). *D*, January 13 at 1820 AKST (14 January at 0320 UTC). *E,* January 13 at 2120 AKST (14 January at 0620 UTC). *F,* January 14 at 0720 AKST (1620 UTC). Date and times in Puff model forecasts are in UTC, and particles are color-coded by elevation a.m.s.l.

from the events on January 13 and 14. Figure 8*A* shows the AVHRR sensor satellite data at 1246 AKST (2146 UTC) on January 13. Here, the first three events from January 13, events 3–5 in table 1, are detected with the reverse absorption method in the satellite data, giving a negative BTD signal. Figure 8*B* shows the Puff forecast at 1250 AKST (2150 UTC), within 5 minutes of the satellite data. Figure 8*C* shows a comparison of the two data sets, by evaluating their spatial footprint. As we were unable to determine ash retrievals and then use the Puff model to predict airborne concentrations, a spatial comparison was the only possible method for data comparison. Here, the "footprint match" between the Puff predictions and the satellite data is emphasized by points labeled 1, 2 and 3 (fig. 8*C*). From the Puff forecasts, the modeled ash at altitudes from 8–10 km a.m.s.l. (26,000–33,000 ft) matches the satellite data. As the ash clouds were detectable in the satellite data using the reverse absorption method and a negative BTD signal, they were termed translucent. Determination of their altitude is only possible from this comparison method with Puff. The Puff

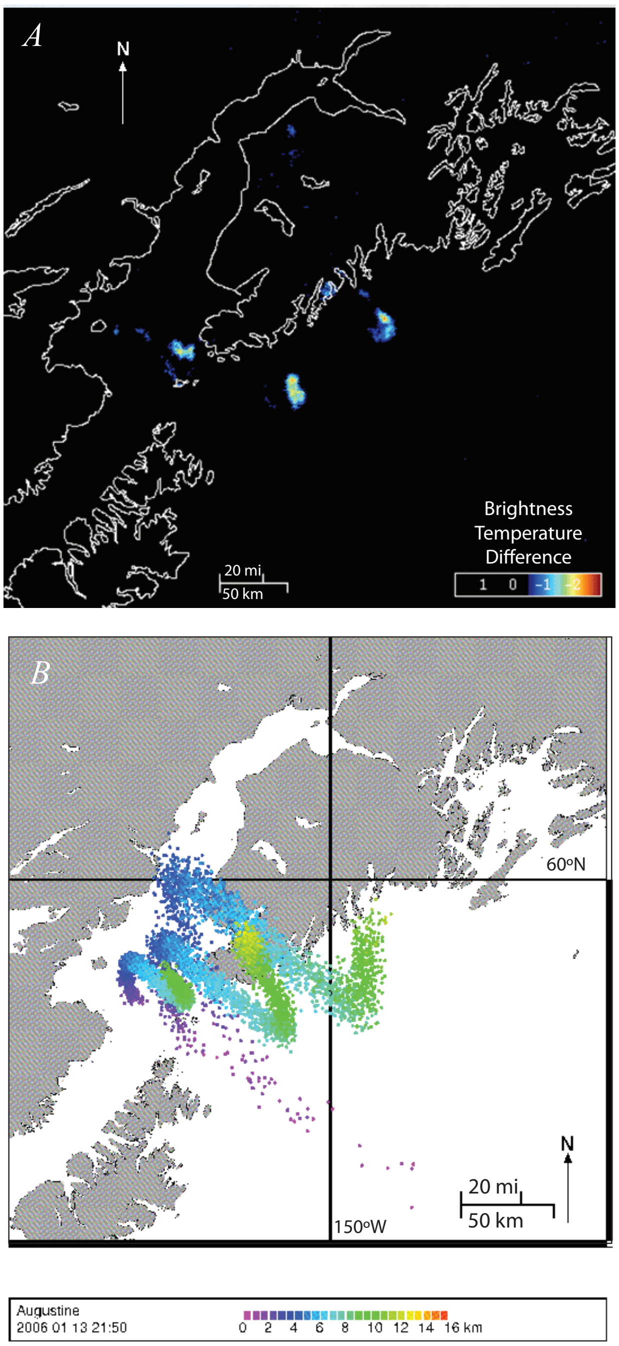

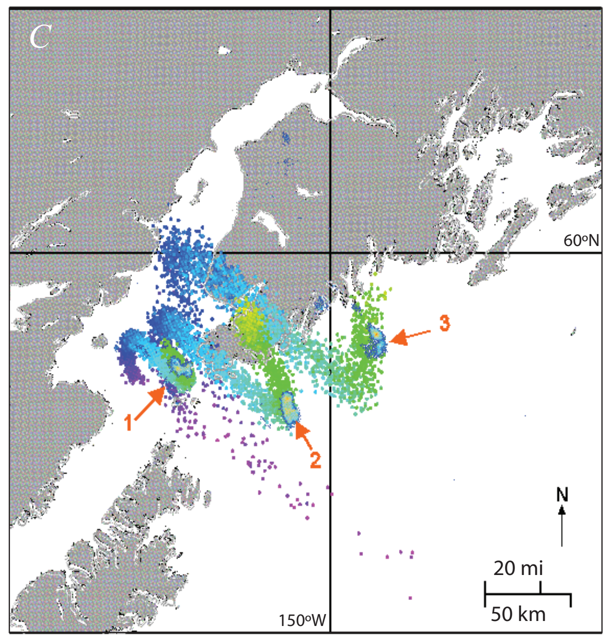

Figure 8. Comparison between Advanced Very High Resolution Radiometer (AVHRR) sensor remote-sensing data and the first three plumes from the January 13–14 explosive events. *A*, AVHRR at 1246 AKST (2146 UTC) on January 13. Brightness temperature difference (BTD) scale is difference in AVHRR channels 4 and 5 using the reverse absorption method. *B*, Puff-eruption response simulation at 1250 AKST (2150 UTC). Date and times are in UTC, and particles are color-coded by elevation a.m.s.l. *C*, AVHRR BTD plumes superimposed on the Puff model simulation (Puff plumes match to satellite noted at points 1, 2 and 3).

simulations were able to match the ash cloud movements, even though they showed a larger amount of dispersion. This increased dispersion could be a result of (1) the ash concentrations seen in the modeled cloud being below the detection limits of the reverse absorption technique or (2) in the model forecast, the dispersion factor being set too high.

In the past few years, virtual globes, specifically Google Earth™, have been used for displaying scientific data. They allow the Puff model predictions to be shown in their three-dimensional form. Figure 9 shows both a graphical representation of the Puff model forecast and a three-dimensional view of event 3 on January 13. Figure 9*A* shows the ash cloud's location in a graphical plan view, with no three-dimensional viewpoint. Here, the ash cloud altitudes are shown as color-coded particles from 0 to 16 km a.m.s.l (0 to 52,000 ft). Figure 9*B* shows a three-dimensional viewpoint of the same Puff prediction in Google Earth. Selecting each ash particle in Google Earth, the observer is provided with its location and altitude. In addition, there is a "time stamping option", highlighted within the box in figure 9*B*, which allows an animation of ash cloud movement. This three-dimensional viewpoint and interactive ability is a novel tool for analyzing the dispersion model forecasts, something that is not possible with the graphical map image.

Additional comparison data during the January 13–14 period included ashfall reports in Homer/Port Graham on January 13, as well as Shasta County, California, on January 16 (Wallace and others, this volume) and aerosol data collected in Homer on January 13 (Cahill and others, unpub. data). All reports indicate that ashfall was very light. Figure 8*B* shows the Puff simulation of the low level ash cloud moving towards Homer and the Kenai Pennisula, towards the ashfall reports in Port Graham and aerosol samplers in Homer. In addition, the Puff simulations of the six plumes (fig. 7*F*) show that the forecasted ash clouds could have passed over the northwestern contiguous United States,

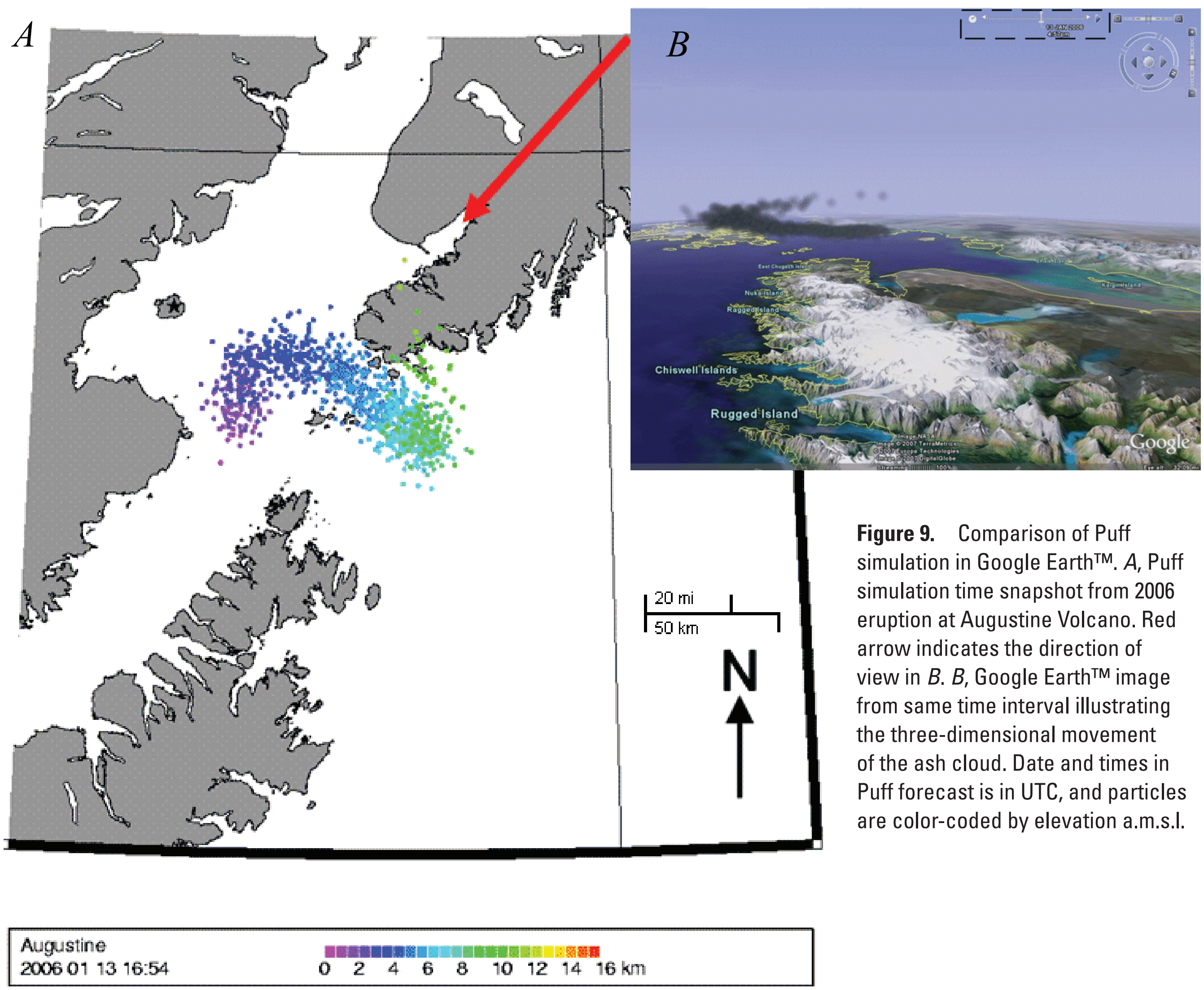

Figure 9. Comparison of Puff simulation in Google Earth™. *A*, Puff simulation time snapshot from 2006 eruption at Augustine Volcano. Red arrow indicates the direction of view in *B*. *B*, Google Earth™ image from same time interval illustrating the three-dimensional movement of the ash cloud. Date and times in Puff forecast is in UTC, and particles are color-coded by elevation a.m.s.l.

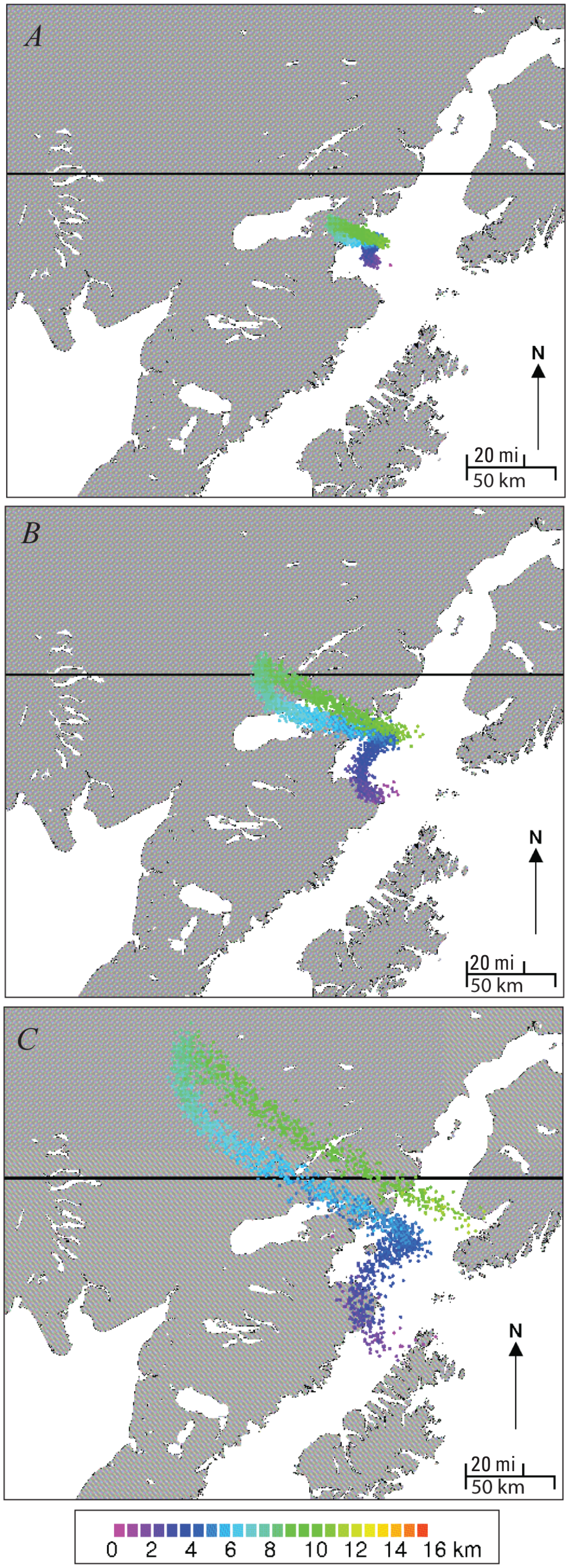

Figure 10. Puff time snapshots following simulation of January 17, 2006 explosive event. *A*, +1 hour or 0858 AKST (1758 UTC). *B*, +3 hours or 1058 AKST (1958 UTC). *C*, +6 hours or 1358 AKST (2258 UTC). Date and times are in UTC, and particles are color-coded by elevation a.m.s.l.

towards the reported ashfall in California. Peterson and others (2010) provide a comparison of the Puff simulations during the events on January 13–14 with those using the HYSPLIT and CanERM VATD models.

January 17, 2006

Following 3 days of relative quiescence, on January 17, 2006, Augustine had a single explosive event starting at 0758 AKST (1658 UTC), and lasting 4 minutes and 11 seconds, with a volcanic ash plume rising to an altitude of approximately 13 to 14 km a.m.s.l (43,000–46,000 ft) (event 9 in table 1). The ash cloud was only detected on 3 AVHRR satellite images (Bailey and others, this volume). Figure 10 shows the Puff model simulations in response to the detected eruption at 1 hour, 3 hours, and 6 hours after the start of the event. Here, the high altitude sections of the ash cloud travel north-northwest, and the low altitude sections travel to the southwest. Figure 11 shows a comparison between the Puff model simulations, the AVHRR satellite sensor data and the NWS Next Generation Radar (NEXRAD). Comparison between the Puff simulation (fig. 11*A*) and the satellite data (fig. 11*B*) show that the detected opaque ash cloud is at 8 to 10 km a.m.s.l (26,000–33,000 ft). The 0300 AKST January 17, 2006 radiosonde sounding collected from Kodiak, King Salmon, and Anchorage stations (http://weather.uwyo.edu/upperair/naconf.html), indicate that the −55.45°C temperature in figure 11*B* corresponds to approximately 8.5 to 9 km a.m.s.l (26,000-30,000 ft), using the altitude-temperature method of Sparks and others (1997) as developed from Kienle and Shaw (1979). NEXRAD, in clear air mode, shows very little reflectivity across Cook Inlet except for signals of +4 to +16 DBZ at Augustine (fig. 11*C)*. The match in timing between the three datasets provides good agreement that (1) the radar was able to detect the ash cloud, (2) the Puff model results matched the satellite data, and (3) the ash cloud was at 8 to 10 km a.m.s.l. (26,000–33,000 ft).

In addition, a retrospective comparison between the Puff predictions and measured ashfall from the January 17 event was used to assess the Puff model's ability to reliably forecast ashfall (fig. 12). Figure 12*A*, adapted from Wallace and others (this volume), shows that ashfall occurred to the northwest of Augustine Volcano towards Lake Iliamna (location is shown in Figure 2). There are also ground observations of ashfall from Iliamna, Pedro Bay, and Nondalton from local citizens. Figures 12*B*–12*D* show the Puff modeled ashfall predictions using three different wind-field datasets: National Centers for Environmental Prediction (NCEP) global reanalysis, WRF 5-km resolution and WRF 1.67-km resolution. For the reanalysis wind-field data (fig. 12*B*), the Puff-forecast ashfall occurs mostly over Cook Inlet. Although no ashfall samples were collected, there were ashfall reports at Port Graham, and the reanalysis forecast suggests that it could have been from this eruption, on the basis of a few predicted ashfall particles in the area. Because Puff is a tracer model, ashfall amounts can be simulated only relative to other locations, but light ashfall would be consistent with the model prediction.

Using the higher spatial resolution wind-field data from WRF, figures 12*C* and 12*D* show a very different ashfall pattern. Figure 12*C* predicts ashfall north of the volcano towards Pedro Bay and north-west towards Port Graham. Figure 12*D* predicts ashfall both southeast over the ocean and northwest towards Lake Iliamna (its location is shown in figure 2). This 1.67-km spatial resolution wind field was an experimental dataset used during the eruption, and as a result its spatial domain doesn't extend much beyond 20 km from the volcano. A larger domain at this finer spatial resolution could have resulted in a better match between the Puff model forecasts and the ashfall reports and measurements shown in figure 12*A*. The Puff model uses the wind field for its advection term, and the speed and direction for all particles is determined from the wind-field model data. A coarse resolution wind-field dataset requires interpolation to determine the wind field for each ash particle. Finer grids require less interpolation and hence more accurate representation of the actual atmospheric conditions.

This retrospective analysis suggests that an area like Cook Inlet, which has complex winds due to surrounding mountainous terrain and numerous valleys open to the ocean, requires higher resolution wind fields to better model the atmospheric boundary layer. This could result in more accurately modeled volcanic ashfall, an important factor for producing volcanic ashfall advisories in volcanic crises. Other factors, such as size distribution, aggregation, and deposition processes can also affect ashfall forecasts. However, a better representation of the wind field in the model's advective term will provide an improved forecast for both airborne ash movement and ashfall. Figures 10 through 12 have shown that the Puff model was able to match both the

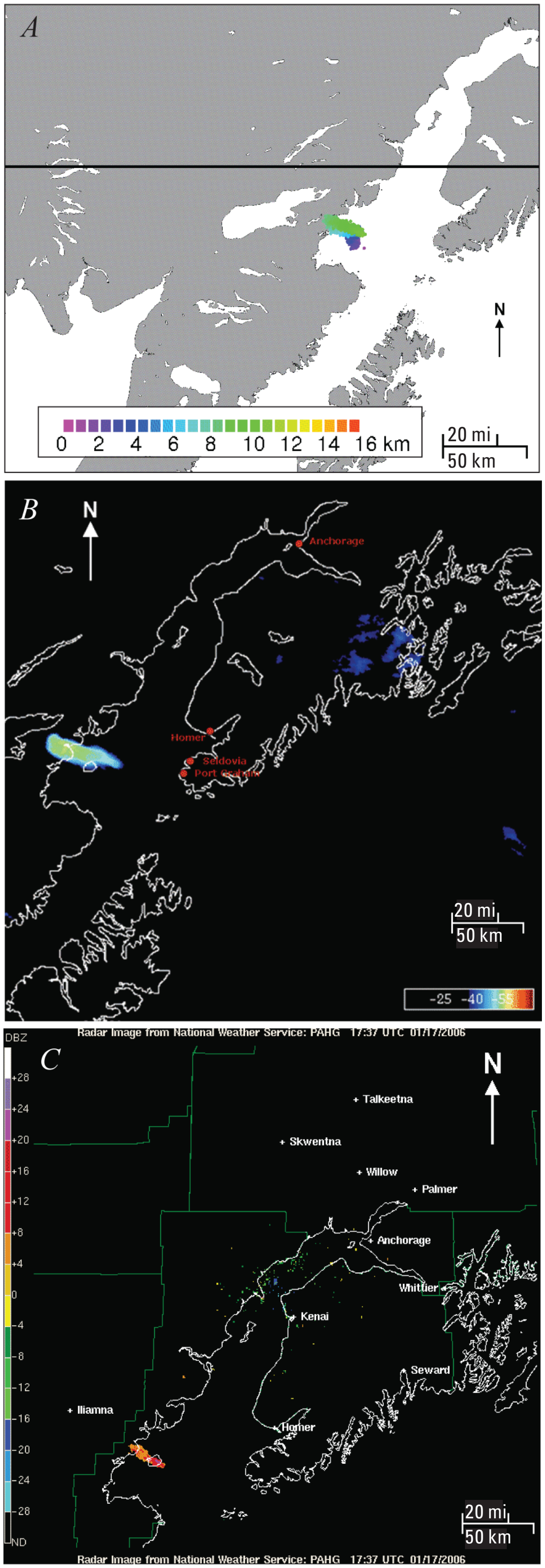

Figure 11. Three views of the January 17, 2006, explosive event. *A*, Puff model output from 0838 AKST (1738 UTC). Times are in UTC, and particles are color-coded by elevation a.m.s.l. *B*, Advanced Very High Resolution Radiometer single channel satellite data from 0838 AKST (1738 UTC), showing cold temperatures of the infrared spectrally opaque ash cloud. *C*, NEXRAD radar from 0837 AKST (1737 UTC).

radar and satellite data for the January 17 event, but they also show how higher resolution wind-field data are needed for the Puff model to provide reliable forecasts of ashfall. After this single event on January 17, the next events occurred on January 28 and led to the continuous eruptive phase from January 28 to February 10, 2006, with declining vigor from February 2 to 10.

January 28 to February 2, 2006

On January 27–28, 2006, at 2024 to 0742 AKST Augustine Volcano again produced several explosions (events 10–13 in table 1), lasting as long as 9 minutes with ash plumes varying from 3 to 9 km (10,000–30,000 ft) a.m.s.l. that dispersed to the southeast and south-southwest.

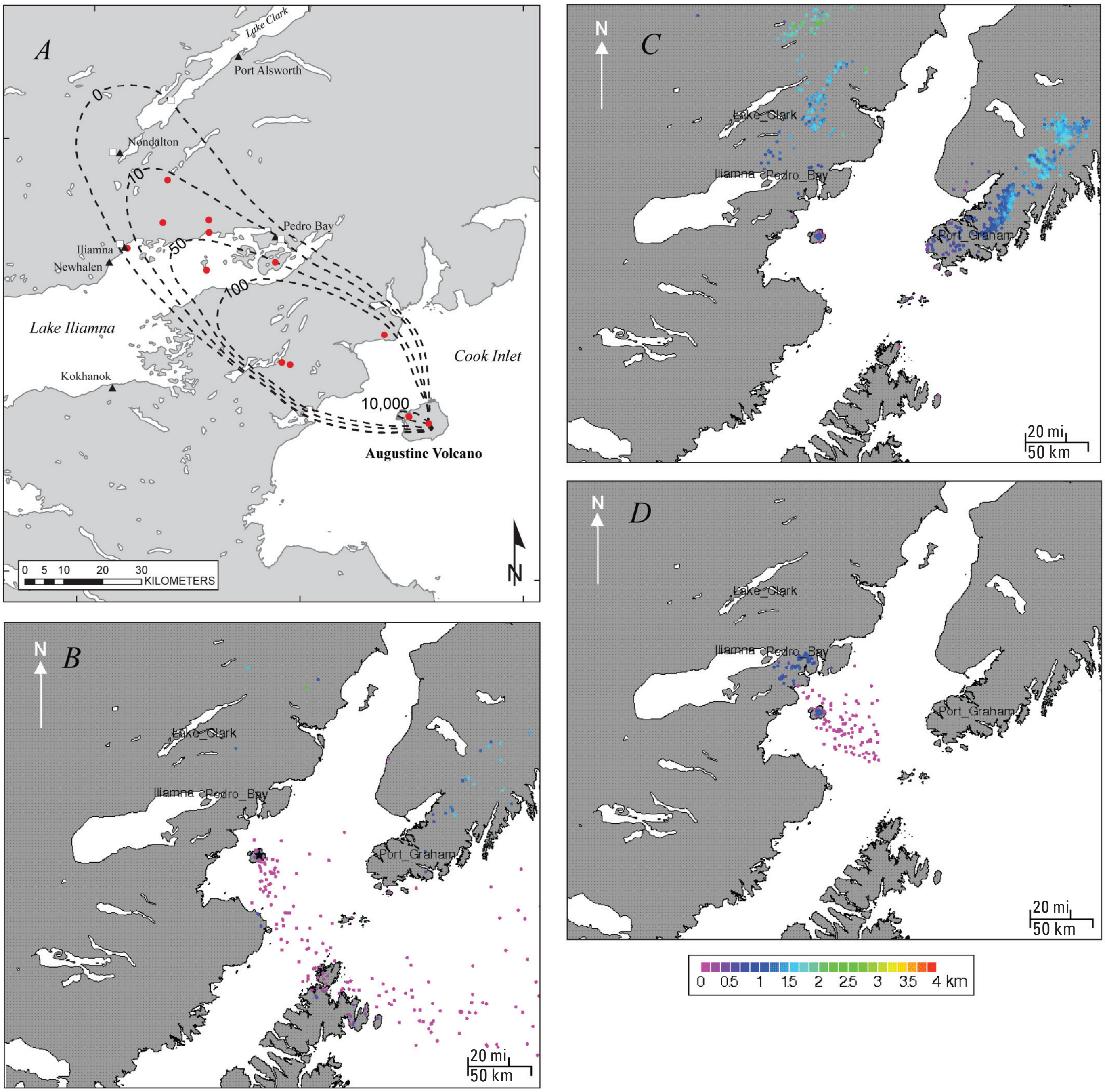

Figure 12. Measurements and simulations of ashfall from January 17, 2006 event. *A,* Ashfall isopach in g/m^2, (from Wallace and others, this volume). *B,* Puff model simulated ashfall from post event analysis with NCEP reanalysis wind field. *C,* Puff model simulated ashfall from post event analysis with WRF 5-km resolution wind field. *D*, Puff model simulated ashfall from post event analysis with WRF 1.67-km resolution wind field. Ashfall particles are color-coded by ground elevation a.m.s.l.

Then the volcano was relatively quiet for several hours from 0742 AKST (1642 UTC) until around 1430 AKST (2330 UTC), when seismicity began to increase. This led to the continuous phase as seen in the NEXRAD radar, which immediately started to detect a signal over the volcano, from ash emission, that continued for several days (D. Schneider, written communication (2006) and AVO Logs). Over the continuous phase, ash clouds reached approximately 3 to 4.5 km a.m.s.l (10,000–15,000 ft), with discrete events reaching 7.3 km (24,000 ft) (table 1). For the period from January 28, 2006, onwards, Puff used an initial 5 km (~16,500 ft) a.m.s.l ash plume and forecast wind fields from the NAM 216 model domain. To make the best use of the forecast data, the model was run for an initial 24 hours (from 1430 AKST/2330 UTC on January 28, 2006) and then restarted for another 24 hours, continuing in this way until February 2. Each new model run used the most recent forecast wind fields. Figure 13 is an example of the ash signal as detected from the BTD signal using the AVHRR satellite remote-sensing data on January 28 at 1731 AKST (January 29 at 0231 UTC). There is a very strong negative BTD signal to the south of the volcano across Kodiak Island. Additional discussion of the satellite data is included in Bailey and others (this volume).

At the beginning of the continuous phase, the synoptic conditions showed that volcanic material would initially move towards the southeast and then curve rapidly around with a northerly heading and be transported rapidly to the Alaska interior (Webley and others, 2008). Figure 14, adapted from Webley and others (2008), shows daily AVHRR and MODIS sensor data composites of the ash clouds from January 29 to 31. The movement of the ash clouds was initially in a southerly or south-easterly direction on January 28, shifting to a more southerly direction by January 29, then an easterly direction on January 30, and a northeasterly direction by January 31. These observations support Puff forecasts for this time period (fig. 15). Volcanic ash concentrations eventually receded to levels below the detection limits of the satellite data, with no ash clouds detected beyond the Cook Inlet area.

For the period from January 29 to February 1, the Puff predictions showed an ash-cloud trajectory towards Kodiak Island (fig. 15*A*) with a subsequent rotation to the northeast and across the Kenai Peninsula by the following day (fig. 15*B*). By the third day, predictions indicated a northeasterly trajectory (fig. 15*C*). Aerosol samples, from an eight stage impactor (described in Cahill, 2003) were collected at Homer, Alaska, and confirmed the presence of ash "at ground level there." These provide ground-based verification to go with the airborne ash detection (fig. 14) of the ash within Cook Inlet. Lidar measurements from three distinct systems across Alaska were also used to aid in confirming the Puff-model-predicted volcanic ash clouds from the continuous period (Sassen and others, 2007; Webley and others, 2008). The lidar measurements at two sites were collected in response to the Augustine volcanic activity and Puff simulations. Lidar detected the ash cloud under both clear skies and partially cloudy conditions. The characteristics of the volcanic ash were distinct from those of the atmospheric clouds. Figure 16 shows the Puff model prediction at 1900 AKST, January 31 (0400 UTC, February 1), during the acquisition of the lidar data at one station, as described in Webley and others (2008).

The lidar data confirmed the presence of the volcanic cloud overhead at Fairbanks, Alaska, and also confirmed the independent motion of the upper and lower level ash clouds. The location of the ash cloud in figure 16 shows ash passing over Fairbanks (marked as "F"). Aerosol analysis showed that ratios of iron to calcium at both Homer and Fairbanks indicated to a similar source and under "normal conditions" such ratios would not have been recorded at Fairbanks (Cahill and others, unpub. data). Figures 15*C* and 16 show that Puff-predicted ash clouds would have passed over Homer and

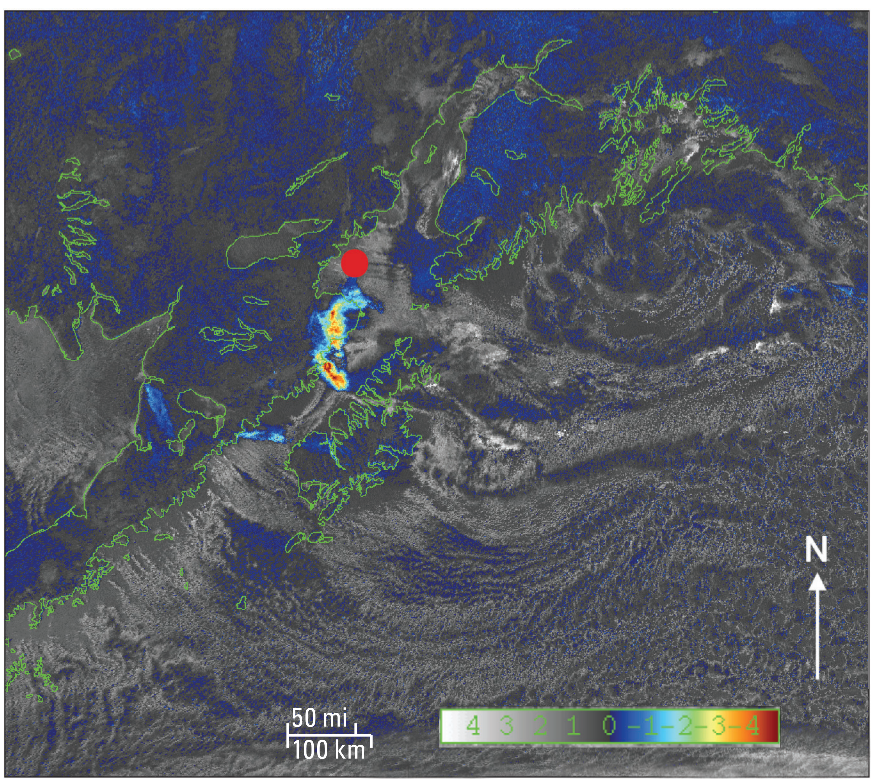

Figure 13. Advanced Very High Resolution Radiometer brightness temperature difference satellite data from January 28, 2006, at 1731 AKST (January 29, at 0231 UTC) showing the ash signal as detected through the reverse absorption method. Here, the ash is shown as a negative BTD signal. Location of the volcano is show by the red circle.

Fairbanks at the times the aerosol data were collected. The measurements of the aerosol signals in the lidar returns provided a unique confirmation tool to the Puff predictions.

The continuous phase of the eruption provided some unique validation opportunities for the Puff model predictions. Webley and others (2008) show the possibilities of lidar being used as a validation tool for volcanology. As shown by Sassen and others (2007), an autonomous lidar could be used by both the meteorological and volcanological communities for eruption crisis monitoring. Lidar measurements as an eruption response tool for volcano monitoring could be applied to known erupting volcanoes as well as the dispersed volcanic material from a much more distant eruption (Webley and others, 2008).

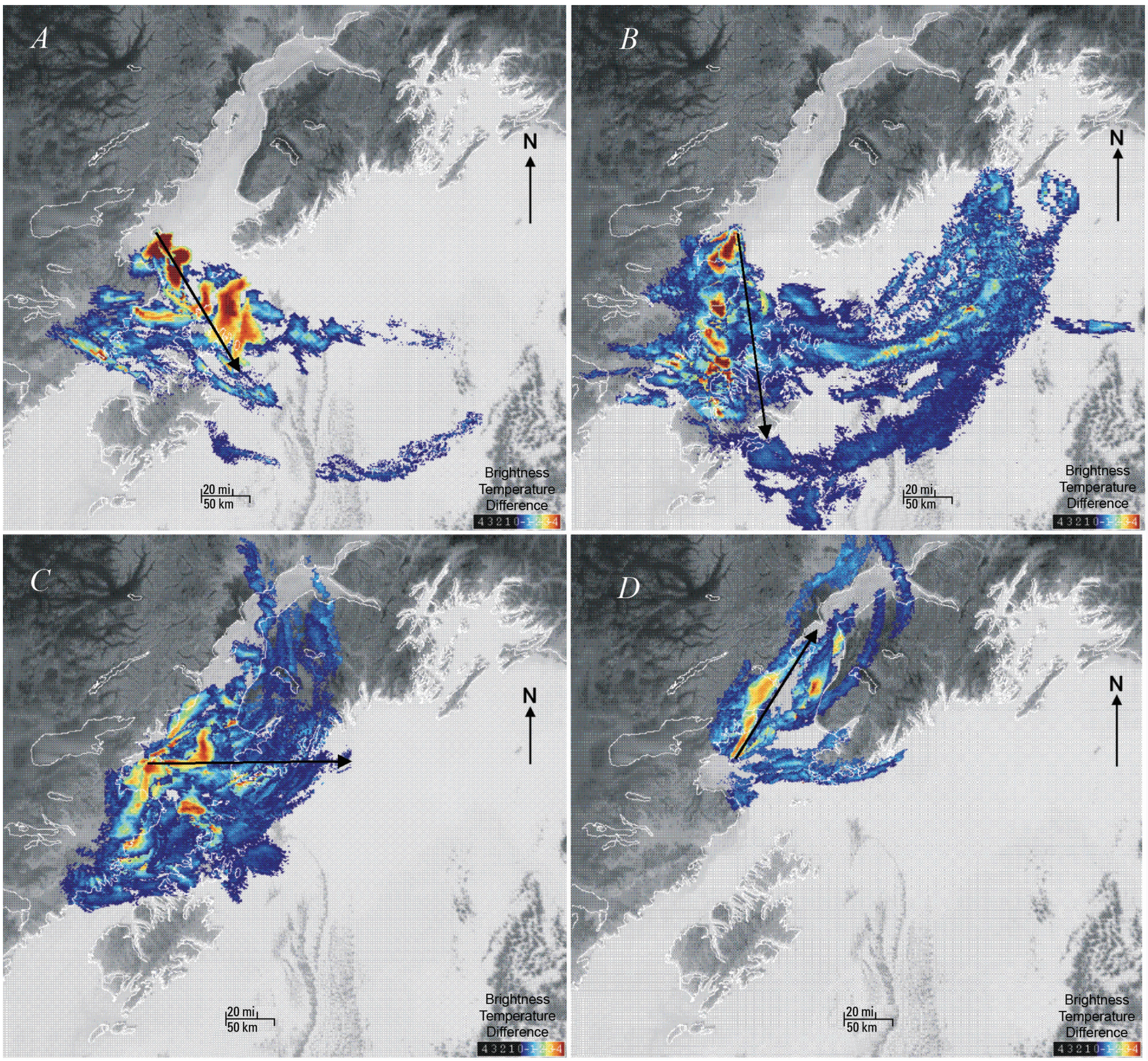

Figure 14 Moderate Resolution Infrared Spectrometer (MODIS) and Advanced Very High Resolution Radiometer data (AVHRR) ash-detection daily composites for (*A*), January 28, (*B*), January 29, (*C*), January 30 and ,(*D*), January 31 2006. Black arrows indicate general direction of ash cloud movement. Adapted from Webley and others (2008). Here, the ash is shown as a negative brightness temperature difference (BTD) signal.

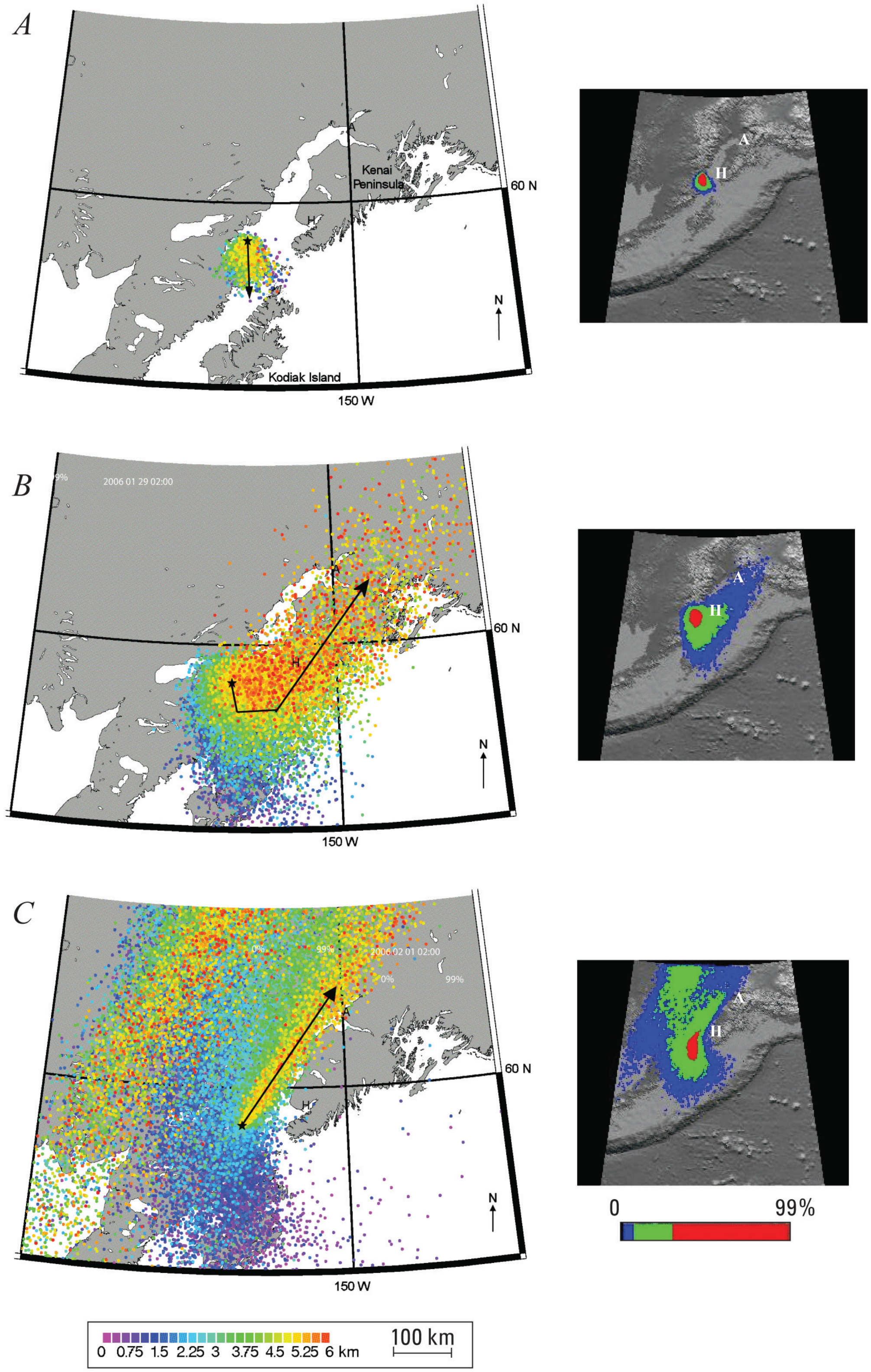

Figure 15. Puff model simulation of ash cloud movement in Cook Inlet during the continuous phase of the 2006 Augustine eruption, adapted from Webley and others (2008). Black arrows show general direction of the ash clouds movement. *A,* January 28 at 1700 AKST (January 29 at 0200 UTC). *B,* January 29 at 1700 AKST (January 30 at 0200 UTC). *C,* January 31 at 1700 AKST (February 1 at 0200 UTC). Date and times in Puff model forecasts are in UTC, and particles are color-coded by elevation. H, Homer; A, Anchorage. Thumbnail shows relative airborne concentration as a percentage of maximum predicted concentration.

Discussion and Conclusions

Volcanic ash clouds are a very real hazard during an eruption, even after the explosive/effusive activity has ended. They can pose a hazard to domestic and international air traffic and affect local communities. Also, they can be tracked over long distances for several days after the end of an eruptive period. The 2006 eruption of Augustine Volcano, Alaska, produced 13 explosive events over a 2-week period, followed by a continuous period of ash emission over several days.

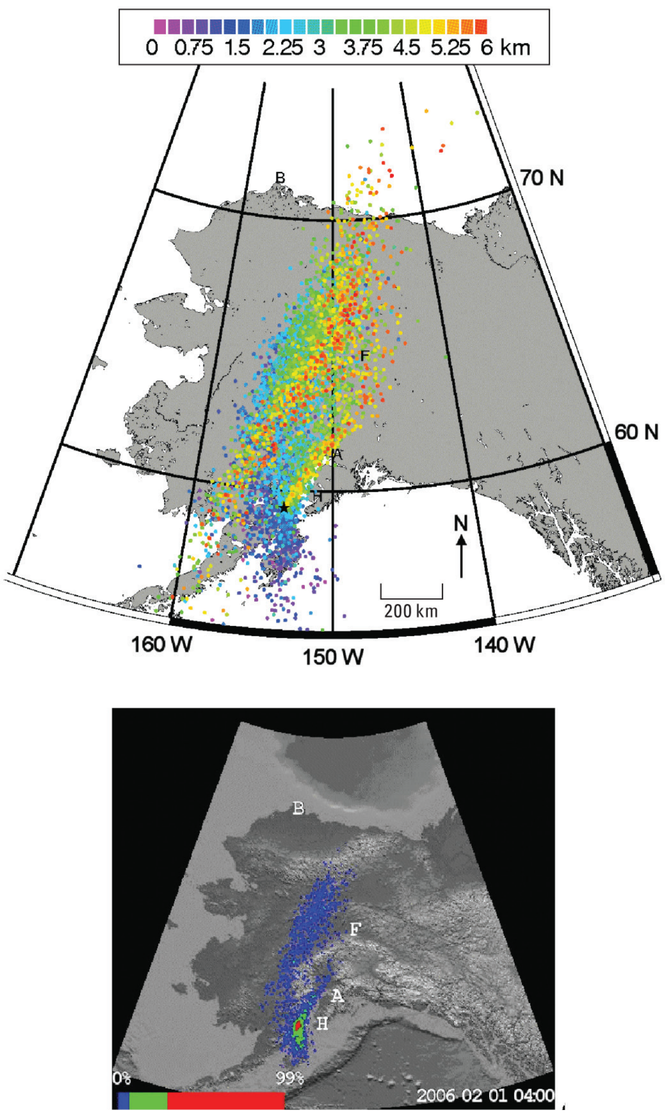

Figure 16. Puff model simulation snapshot on January 31, 2006 at 1900 AKST (February 1, 2006 at 0400 UTC) of ash cloud movement across Alaska mainland that coincided with lidar measurements, from Webley and others (2008). Particles are color-coded by elevation. Black star shows location of Augustine Volcano. H, Homer, A, Anchorage; F, Fairbanks. Lower panel shows relative airborne concentration as a percentage of maximum predicted concentration.

The Puff volcanic ash transport and dispersion model's ability to track multiple volcanic ash clouds was first used for an eruption response during this eruption. Its use was highly successful during the January 13–14 events and compared well with the satellite data (fig. 8). The NWS, with assistance from AVO, produced numerous volcanic ash advisories, and at one point Anchorage airport was affected, as airline flights were cancelled. Predicting the movements of these ash clouds from Augustine was critical to assess the impact they would have on their surroundings. The Puff model was able to provide forecasts of all the ash clouds from the events in table 1. The model's predictions were used during the eruption response by AVO and also the NWS to assess the cloud's movements and the impacts they would have on the aviation community and local residents.

As a result of the enormity of the data obtained during the Augustine eruption, the Google Maps™ application programming interface (API) is now used to display Puff automated predictions for potential eruptions at volcanoes of elevated alert status see Puff Web site (http://puff.images.alaska.edu). Webley and others (2009) provide a detailed description of the automated predictions and the API to all the Puff model predictions for these volcanoes. Virtual Globes are an excellent geographic frame of reference to display model results that can be easily understood. Figure 9 showed how displaying the data in a Virtual Globe provides (1) a better understanding of ash cloud movement and (2) an ability to visualize the data in three dimensions. Additional information, such as satellite and seismic data can be easily added to the Virtual Globe interface.

This paper illustrates the reliability of the Puff model airborne-ash predictions near Augustine Volcano and the distal ash plumes as compared to various other techniques, such as remote-sensing satellite data, aerosol samplers, and the lidar systems. Figure 11 for the January 17 event shows that use of higher spatial resolution wind fields would improve ashfall predictions, especially in a topographically diverse region such as Cook Inlet. Further work on the use of the WRF model for Puff predictions is required, both for airborne ash movement and for ashfall forecasts.

During the 2006 Augustine eruption, a large amount of information was provided by the model predictions. As a result, an improved tool to provide up-to-date analysis and allow quick assessments was required. The new automated predictions, now used by AVO, alleviated the requirement to initiate Puff model runs 24 hours a day, once an eruption was reported. The 5-minute assessment can be made from these automated Puff predictions and then "improved" once more information on the eruption is available. Since the 2006 eruption of Augustine, the Puff model predictions have been used for numerous volcanoes around the world (Webley and others, 2009). They are used by AVO, NWS, AFWA, and KVERT to determine the movement of volcanic eruption clouds in the NOPAC. Further developments for the Puff model will include determining reliable actual airborne volcanic ash cloud concentrations, through model initialization from satellite derived ash retrievals, and to work with the USGS-led eruption source parameters working group (Mastin and others, 2009) to provide improved volcanic ash forecasts by taking account of past eruption history.

Acknowledgments

The authors wish to thank the staff and students in the AVO remote-sensing group for their monitoring of Augustine Volcano and analysis of the remote-sensing satellite data during the eruption response. The authors would like to thank the Arctic Region Supercomputing Center (ARSC) for its support of Webley's and Bailey's postdoctoral fellowships during the eruption crisis. The authors also appreciate the Geophysical Institute at the University of Alaska Fairbanks for their support of the AVO remote-sensing team.

References Cited

Aloisi, M., D'Agostino, M., Dean, K.G., Mostaccio G., and Neri, A., 2002, Satellite analysis and PUFF simulation of the eruptive cloud generated by the Mount Etna paroxysm of 22 July 1998: Journal of Geophysical Research, v. 107, no. B12, doi:10.1029/2001JB000630.

Bailey, J.E., Dean, K.G., Dehn, J., and Webely, P.W., 2010, Integrated satellite observations of the 2006 eruption of Augustine Volcano, *in* Power, J.A., Coombs, M.L., and Freymueller, J.T., eds., The 2006 eruption of Augustine Volcano, Alaska: U.S. Geological Survey Professional Paper 1769 (this volume).

Blong, R.J., 1984, Volcanic hazards: A sourcebook on the effects of eruptions. Sydney. Academic Press, 424 p.

Cahill, C.F., 2003, Asian aerosol transport to Alaska during ACE-Asia: Journal of Geophysical Research, v. 108, no. D23, doi:10.1029/2002JD003271.

Casadevall, T.J., 1993, Volcanic hazards and aviation safety, lessons of the past decade: FAA Aviation Safety Journal, v. 2, p. 1–11.

Casadevall, T.J., and Krohn, D., 1995, Effects of the 1992 Crater Peak eruptions on airports and aviation operations in the United States and Canada: U.S. Geological Survey Bulletin 2139, p. 205–220.

Coombs, M.L., Bull, K.F., Vallance, J.W., Schneider, D.J., Thoms, E.E., Wessels, R.L., and McGimsey, R.G., 2010, Timing, distribution, and volume of proximal products of the 2006 eruption of Augustine Volcano, *in* Power, J.A., Coombs, M.L., and Freymueller, J.T., eds., The 2006 eruption of Augustine Volcano, Alaska: U.S. Geological Survey Professional Paper 1769 (this volume).

Dean, K., Dehn, J. Engle, K., Izbekov, P., Papp, K., and Patrick, M., 2002, Operational Satellite Monitoring of Volcanoes at the Alaska Volcano Observatory: Advances in Environmental Monitoring and Modelling, v. 1, no. 1, p. 3–35.

Draxler, R.R., and Hess, G.D., 1997, Description of the Hysplit-4 modeling system: NOAA Technical Memo ERL ARL-224, 24 p.

Draxler, R.R., and Hess, G.D., 1998, An overview of the Hysplit 4 modeling system for trajectories, dispersion and deposition: Australian Meteorological Magazine, v. 47, p. 295–308.

Hufford, G.L., Salinas, L.J, Simpson, J.J., Barske, E.G., and Pieri, D.C., 2000, Operational Implications of airborne volcanic ash: Bulletin of the American Meteorological Society, v. 81, no. 4, p. 745–755.

Kienle, J., and Shaw, G.E., 1979, Plume Dynamics, thermal energy and long distance transport of Vulcanian eruption clouds from Augustine Volcano, Alaska: Journal of Volcanology and Geothermal Research, v. 6, no.1–2, p. 139–164.

Krotkov, N.A., Torres, O., Seftor, C., Krueger, A.J., Kostinski, A., Rose, W.I., Bluth, G.J.S., Schneider, D. and Schaefer., S.J., 1999, Comparison of TOMS and AVHRR volcanic ash retrievals from the August 1992 eruption of Mt. Spurr: Geophysical Research Letters, v. 26, no. 4, p. 455–458.

Mastin, L.G., Guffanti, M., Servranckx, R., Webley, P.W, Barsotti, S., Dean, K., Denlinger, R., Durant, A., Ewert, J.W., Gardner, C.A., Holliday, C., Neri, A., Rose, W.I., Schneider, D., Siebert, L., Stunder, B., Swanson, G., Tupper, A., Volentik, A., and Waythomas, C.F., 2009, A multidisciplinary effort to assign realistic source parameters to model of volcanic ash-cloud transport and dispersion during eruptions Mastin, Larry, and Webley, Peter, eds., *in* Special Issue on Volcanic Ash Clouds: Journal of Volcanology and Geothermal Research, v. 186, no. 1–2, p. 10–21. doi:10.0116/j.volgeores.2009.01.008.

McNutt, S.R., Tytgat, G., Estes, S.A., and Stihler, S.D., 2010, A parametric study of the January 2006 explosive eruptions of Augustine Volcano, using seismic, infrasonic, and lightning data, *in* Power, J.A., Coombs, M.L., and Freymueller, J.T., eds., The 2006 eruption of Augustine Volcano, Alaska: U.S. Geological Survey Professional Paper 1769 (this volume).

Miller, T.P., and Casadevall, T.J., 2000, Volcanic ash hazards to aviation. In: Sigurdsson, H., ed., Encyclopedia of Volcanoes: San Diego, Academic Press, p. 915–930.

Papp, K.R., Dean, K.G., and Dehn, J., 2005, Predicting regions susceptible to high concentrations of airborne volcanic ash in the North Pacific region: Journal of Volcanology and Geothermal Research. v. 148, p. 295–314.

Paskievitch, J., Read, C., and Parker, T., 2010, Remote telemetered and time-lapse cameras at Augustine Volcano, *in* Power, J.A., Coombs, M.L., and Freymueller, J.T., eds., The 2006 eruption of Augustine Volcano, Alaska: U.S. Geological Survey Professional Paper 1769 (this volume).

Peterson, R., Webley, P.W., D'Amours, R., Servranckx, R., Stunder, R., and Papp, K., 2010, Volcanic ash transport and dispersion models, *in* Dean, K.G., and Dehn, J., eds., Monitoring volcanoes in the North Pacific—observations from space: Springer Praxis, London.

Power, J.A., Nye, C.J., Coombs, M.L., Wessels, R.L., Cervelli, P.F., Dehn, J., Wallace, K.L., Freymueller, J.T., and Doukas, M.P., 2006, The reawakening of Alaska's Augustine Volcano: Eos (American Geophysical Union Transactions), v. 87, no. 37, p. 373–377.

Prata, A.J., 1989a, Infrared radiative transfer calculations for volcanic ash clouds: Geophysical Research Letters, v. 16, p. 1293–1296.

Prata, A.J., 1989b, Observations of volcanic ash clouds in the 10-12 µm window using AVHRR/2 data: International Journal of Remote Sensing, v. 10, p. 751–761.

Prata, F., Bluth, G., Rose, W., Schneider, D., and Tupper, A., 2001, Comments on "Failures in detecting volcanic ash from a satellite-based technique": Remote Sensing of Environment, v. 78, p. 341–346.

Pudykiewicz, J., 1988, Numerical simulation of the transport of radioactive cloud from the Chernobyl nuclear accident: Tellus, v. 40B, p. 241–259.

Pudykiewicz, J., 1989, Simulation of the Chernobyl dispersion with a 3-D hemispheric tracer model: Tellus, v. 41B, p. 391–412.

Rose, W.I., Delene, D.J., Schneider, D.J., Bluth, G.J.S., Krueger, A.J., Sprod, I., McKee, C., Davies, H. L., and Ernst, G.G.J., 1995, Ice in the 1994 Rabaul eruption cloud; implications for volcano hazard and atmospheric effects: Nature, v. 375, p. 477–479.

Sassen, K., Zhu, J., Webley, P.W., Dean, K., and Cobb, P., 2007, Volcanic ash plume identification using polarization lidar; Augustine eruption, Alaska: Geophysical Research Letters. v. 34, no. 8, doi: 10.1029/2006GL027237.

Searcy, C., Dean, K.G., and Stringer, W., 1998, PUFF; A volcanic ash tracking and prediction model: Journal of Volcanology and Geothermal Research, v. 80, p. 1–16.

Simpson, J.J., Hufford, G., Pieri, D., and Berg, J., 2000, Failures in detecting volcanic ash from satellite based technique: Remote Sensing of Environment. v. 72, p. 191–217.

Simpson, J.J., Hufford, G., Pieri, D., and Berg, J., 2001, Response to Comments on "Failures in detecting volcanic ash from satellite based technique": Remote Sensing of Environment, v. 78, p. 347–357.

Sparks, R.S.J., Bursik, M.I., Carey, S. N., Gilbert, J.E., Glaze, L., Sigurdsson, H. and Woods, A. W., 1997, Volcanic Plumes: Chichester, Wiley, 589 p.

Tanaka, H.L., 1994, Development of a prediction scheme for volcanic ash fall from Redoubt Volcano, Alaska *in* Proceedings of the First International Symposium on Volcanic Ash and Aviation Safety: U.S. Geological Survey Bulletin, 2047, p. 283–291.

Wallace, K.L, Neal, C.A., and McGimsey, R.G., 2010, Timing, distribution, and character of tephra fall from the 2005–2006 eruption of Augustine Volcano, Alaska, *in* Power, J.A., Coombs, M.L., and Freymueller, J.T., eds., The 2006 eruption of Augustine Volcano, Alaska: U.S. Geological Survey Professional Paper 1769 (this volume).

Waythomas, C.F., Dorava, J. M., Miller, T. P., Neal, C. A., and McGimsey, R. G., 1998, Preliminary volcano-hazard assessment for Redoubt Volcano, Alaska: U.S. Geological Survey Open-File Report OF 98-0857, 40 p.

Webley, P.W., Dean, K., Collins, R., Fochesatto, J., Sassen, K., Atkinson, D., Cahill, C., and Prata, A., 2008, Predicting and validating the tracking of a volcanic ash cloud during the 2006 eruption of Mt. Augustine Volcano: Bulletin of American Meteorological Society. v. 89, no. 11, p. 1647–1658 doi: 10.1175/2008BAMS2579.1.

Webley, P.W., Dean, K., Bailey, J.E., Dehn, J., and Peterson, R., 2009, Volcanic ash modeling for North Pacific volcanoes automated operational monitoring and virtual globes, *in* Aviation Hazards from Volcanoes: Natural Hazards, special issue v. 51, no. 2, p. 345–361 doi:10.1007/s11069-008-9246-2.

Wen, S., and Rose, W.I., 1994, Retrieval of sizes and total masses of particles in volcanic clouds using AVHRR bands 4 and 5: Journal of Geophysical Research, v. 99, p. 542–5431.